Article

Thermodynamic and Kinetic Equilibrium for Adsorption of Cellulosic Xylose of Commercial Cation-Exchange Resins

Jiraporn Phojaroen, Marisa Raita, Verawat Champreda, Navadol Laosiripojana, Suttichai Assabumrungrat, and Santi Chuetor*

Cite This: ACS Omega 2024, 9, 3006−3016

Read Online

ACCESS | Metrics & More | Article Recommendations

ABSTRACT: The development of low-cost purification technology is an indispensable need for industrial biorefinery. Xylose is easily obtained from hydrothermal pretreatment of lignocellulosic biomass. This current study emphasizes the chromatographic monosaccharide separation process using commercial cation-exchange resins (CER) including Amberlite 120 and Indion 225 to separate xylose from a mixture of hydrolysates. To understand the performance of the two CER, the studies of equilibrium, thermodynamics, and kinetics were evaluated. In this study, with different xylose concentrations, the adsorption equilibrium was found to follow the Freundlich isotherm model well ($R^2 > 0.90$ for both CER). The results indicated that a pseudo-second-order model represented the xylose adsorption kinetics. In addition, the activation energy of xylose adsorption onto both CER, i.e., Amberlite 120 and Indion 225 was 34.9 and 87.1 kJ/mol, respectively. The present adsorption studies revealed the potential of these commercial CER to be employed as effective adsorbents for monosaccharide separation technology.
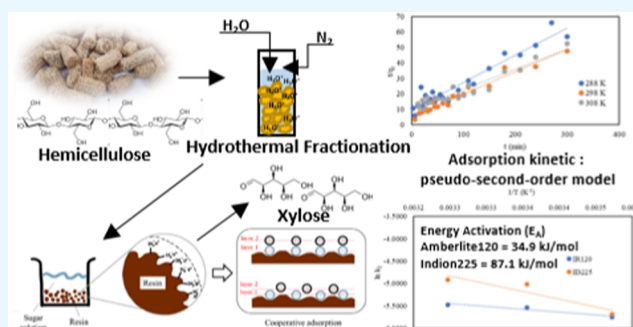
1. INTRODUCTION

The rise in population directly affects the requirement of high global energy consumption. The continuous use of conventional energy resources, such as coal, petroleum, and natural gas, generates greenhouse gases (GHGs) and has high contribution to the global warming phenomenon. The COP26 conference assembled all nations around the world to tackle climate change. One of the important goals of this conference was to accelerate the phase-out of coal utilization and to encourage investment in renewables. The bioresources are considered renewable resources, which have the potential to produce several biobased products such as biofuels, biochemicals, and biomaterials through biorefinery processes. Lignocellulosic biomass being a promising renewable resource can be utilized for producing various high-value-added products. Different biomolecules including cellulose, hemicellulose, and lignin are the important biopolymers that can be converted to useful biobased chemicals. However, the utilization of this material is inadequate because of its recalcitrant structure and low bioconversion. A crucial process in biorefinery is a pretreatment process, which is typically employed to alter the complex structure of lignocellulosic material to release all the biomolecules for further applications.[1−3] Different pretreatment technologies have their own advantages and drawbacks that affect the bioconversion of lignocellulosic material directly.

The hydrothermal pretreatment is commonly a thermo-chemical conversion process, which operates by using water as medium to decompose the lignocellulosic structure, thereby providing a complex liquid fraction called hydrolysate.[4] The chemical reaction taking place in the hydrothermal process is mostly hydrolysis by disrupting and solubilizing the hydroxyl groups of hemicellulose and some specific chemical bonds.[5] The biomass hydrolysate consists typically of monosaccharides, organic acids, phenolic compounds, furfurals, inhibitors, and some other derivatives.[6,7] Monosaccharides are the major components contained in the hydrolysate, which could be useful for conversion into biofuels, biochemicals, food, and pharmaceutical ingredients.[8] The separation and purification methods are thus crucial steps in the downstream processes in a biorefinery to purify or recover pure monosaccharides for further applications. The large amount of pentose sugars such as xylose and arabinose and minor hexose including glucose and mannose are typically produced from the hydrothermal process, which must be separated individually for further use.[9]

The hydrolysate obtained from hydrothermal pretreatment contains typically pentose (C_5) sugars in particular xylose and arabinose depending on the plant species and its operating conditions. The hydrolysate contains some of hemicellulose derivatives such as 5-hydroxymethylfurfural (5-HMF), levulinic acid (LA), and furfuryl alcohol.[6,7,10] The pentose (C5) can be a useful chemical for high-value-added products such as xylooligosaccharides (XOs), xylitol, D-xylose sweetener, intermediate pharmaceuticals, and bioethanol.[11] The use of xylose is commonly large in terms of sugar platform compounds for further applications.[12] Moreover, xylose is an alternative high-value-added sweetener with anticariogenic properties, which are of great concern both for the food and biochemical industries.[13−15] The critical process in the production of the xylose-based molecules is the purification of the xylose from the hydrolysate itself.

There have been several separation techniques developed to separate monosaccharides, such as adsorption by cation-exchange resin or anion-exchange resin, membrane filtration, crystallization, and electrochemical techniques.[16] The development of separation and purification downstream processes integrated into the biorefinery is necessary with an eco-friendly approach and economic feasibility. Nowadays, several separation techniques have been integrated into the downstream process; however, they are of high cost. Therefore, the development of the downstream separation process should be an economically feasible and recyclable process for sustainable future utilization. Membrane filtration is one of the common techniques used for monosaccharide separation such as raw sugar juice, fructooligosaccharides, enzymatic sugars, and fermented sugars.[17] On the other hand, the adsorption technique has been proven to effectively separate monosaccharides in particular cation-exchange resin.[18−20] Liquid chromatography is broadly a potential method of separation of saccharides from the biomass hydrolysate. In chromatography, ion-exchange resins are generally used as adsorbents.[21] Han et al. investigated using 335 gel-type anion-exchange resin to remove the xylose and acetic acid in the liquid hydrolysate of hydrothermally pretreated corncob.[22] The chromatographic separation method of saccharides using ion-exchange resins widely provides a manufacturing process in which the resin is used as a selective medium to separate dissolved compounds from each other.[23−25] Several commercial resins have become popular in the chromatographic separation of sugars.[8] Jiang et al. investigated the use of Amberlite 732 strong acid styrene CER and Amberlite FPA53 anion exchange to integrate the XOS production from bamboo, which enhanced the purity of XOS approximately 92.3%.[26] The effectiveness of sugar separation obtained from hydrolysates can be enhanced by their adsorption onto polymeric adsorbents.[27] Vegas et al. claimed that the use of commercial adsorbents, i.e., Amberlite IRA 400 and Amberlite IRA96, could separate 9.1 and 74.7% of the monosaccharides and oligosaccharides, respectively. Nobre et al. revealed that using an ion-exchange technique could purify the fructooligosaccharides from the steam explosion pretreatment process.[28] Table 1 summarizes the potential of chromatographic sugar separation, which can be implemented to industrial-scale production.[29] Although cation-exchange resin shows its effectiveness for the separation technique, several previous studies do not evaluate its efficacy on biomass hydrolysate.[30] The deficiency in understanding the mechanism of monosaccharides obtained from the hydrothermal process persists.

Table 1. Summary of Liquid Chromatographic Sugar Separation for Different Biomasses

biomass source, country	targeted compounds	initial processing	liquid chromatography mode and operating conditions	notes	refs
spruce and pine cutter saw dust, Finland	monosaccharides (glucose, xylose)	concentrated acid lignocellulosic hydrolysis	laboratory-scale ion-exclusion chromatography, water as the mobile phase, multicolumn with internal recycling	recovery yield and purity were 85 and 95%, notable recovery for acids used in hydrolysis, eluent consumption was 20× lower compared to 4 parallel columns	32
wheat straw, Italy and Switzerland	monosaccharides (glucose, xylose)	pretreatment technique GREG (GReen Ethylene Glycol) by Italian company Biochemtex	laboratory-scale ion-exclusion chromatography, water as the mobile phase	baseline separation between sugars and electrolytes	33
pine branches, China and Japan	monosaccharides (glucose, xylose)	lignocellulosic biomass hydrolysis	laboratory-scale ion-exclusion chromatography with cation resin Amberlite IRP69 (Ca^{2+}), water as the mobile phase	purity of up to 88% for xylose, scaling-up will be a challenge in the presence of higher abundance sugars	34
rice straw, China	monosaccharides (glucose, xylose, and phenolics)	hydrolysis by high-temperature hydrothermal liquefaction	laboratory-scale ion-exclusion chromatography with strong acid cation-exchange resin Amberlite IR120 (Na^+), water as the mobile phase	higher adsorption selectivity between phenol and glucose compared to resin with Ca^{2+} form	35
pine branches, China	monosaccharides (glucose, xylose) and organic acids	hydrolysis by low-temperature hydrothermal liquefaction	laboratory-scale ion-exchange chromatography with a weak anion-exchange resin Amberlyst A21, sodium hydroxide solutions as the mobile phase	rapid separation of sugars and acids, different selectivity from ion exclusion chromatography, large adsorption capacity of column	35

Moreover, the CER in particular Amberlite is usually applied for sugar decolorization in the sugar industry.[26,31]

To our knowledge, there is paucity of information on how to separate and purify xylose, glucose, and arabinose from the lignocellulosic hydrolysate. Besides, the design of industrial-scale chromatographic separation to be integrated into the biorefinery process begins with the selection of a suitable adsorbent material and understanding the thermodynamic properties and kinetic adsorption. This work studied the adsorption equilibrium, thermodynamics, and kinetics of two commercial CER including Amberlite IR120 and Indion 225 for separation of xylose from single synthetic monosaccharides (xylose, arabinose, and glucose). Both commercial CER were selected due their availability and local supply. Moreover, these two commercial resins have strong capability of separating the monosaccharides and low costs. Studies on the thermodynamics properties of sugars, furans, and other components existing in hydrolysates have not been done with these two CER yet.[7,10] The studies would provide valuable information for the selection of a cheap and effective adsorbent and the design of chromatographic separation processes integrated to the downstream process of large-scale biorefinery.

2. MATERIALS AND METHODS

2.1. Materials and Chemicals. Corncob (CC) was provided from local farmers in Maetha District, Lampang Province, Thailand. CC was oven-dried until the moisture content was constant approximately 8−10% and coarsely ground by knife milling to obtain a particle size of 2−4 mm. Samples for hydrothermal pretreatment were sieved approximately to a particle size of 1 mm.

The CER Amberlite IR120 in H+ form was purchased from Filter Supply Co., Ltd., Muang Nonthaburi District, Nonthaburi Province, Thailand. Indion 225 in H+ form was kindly supplied by Ion Exchange India Ltd. The properties of both CER are presented as seen in Table 2.

Table 2. Properties of the Both Commercial CER

Indion 225	Amberlite IR120
matrix: polystyrene	matrix: styrene divinylbenzene copolymer
ionic form as supplied: H+	ionic form as supplied: H+
total exchange capacity: 1.8 mequiv/mL	total exchange capacity: ≥1.80 equiv/L
functional group: sulfonic acid	functional group: sulfonic acid
particle size range: 0.3−1.2 mm	particle size uniformity coefficient: ≤1.8 mm
effective size: 0.45−0.55 mm	harmonic mean size: 0.62−0.83 mm
	<0.300 mm 2% max

2.2. Analytical Method. Chemical compositions of hydrolysate and monosaccharides were quantified by using high-performance liquid chromatography (HPLC) (Shimadzu with UV-detector and RI detector). Before injection, the hydrolysate was filtered through a 0.22 μm filter. The monosaccharide analysis was conducted using an Aminex HPX-87H column, using a 5 mM concentration of the sulfuric acid aqueous solution as the mobile phase at a flow rate of 0.5 mL/min. The column temperature was maintained at 65 °C.

2.3. Hydrothermal Pretreatment. CC was pretreated by using a hydrothermal technique without using a catalyst. 30 g of CC was dissolved in 300 mL of distilled water in a Parr reactor (1L) at different temperatures (165−180 °C) and for

four different time durations (10, 20, 30, and 40 min) under 20 bar pressure with N_2 and a rotation speed of 200 rpm. After pretreatment, the CC was divided into a mixture of hydrolysates and solid residues, which were then separated through a filter to obtain its hydrolysate. The hydrolysate was analyzed via high-performance chromatography (HPLC) to optimize the conditions for obtaining maximum xylose content.

2.4. Adsorption Equilibrium. Adsorption equilibrium was investigated through static adsorption. To study the effect of initial concentration, about 0.1 g of two different resins was submerged in 25 mL of synthetic monosaccharide solutions at different concentrations in flasks. The concentrations of glucose, xylose, and arabinose solutions varied in a range of 1−40 g/L. After the resin was dispersed in the solution, the flasks were kept at 25 °C for 24 h in an incubator shaker at 150 rpm. This operational duration (h) was too long enough for the adsorption to reach the equilibrium. The adsorption isotherms were analyzed according to the equilibrium concentration in the liquid phase and the equilibrium adsorption capacity in the solid phase. The adsorption capacity of monosaccharide solutions was estimated using the following equation eq 1[20]

$$q_e = \frac{(C_0 - C_e)V}{m_R} \tag{1}$$

where q_e is the adsorption capacity of the resin at equilibrium, C_0 is the initial monosaccharide concentration in the solution, C_e is the residual monosaccharide concentration in the solution after equilibrium, V is the volume of the solution, and m_R is the amount of resin used.

The study of the effect of adsorbent dosage on the extent of pure xylose and mixed sugars (10 g/L xylose, 0.5 g/L glucose, and 2.5 g/L arabinose) was evaluated with different adsorbent dosages (0.5, 1, 1.5, 2, 2.5, and 3 g) for two different resins. Each adsorbent dosage was added into 50 mL for both the solutions.

2.5. Adsorption Isotherms. To study the adsorption isotherms, 1 g of Amberlite IR120 and 0.2 g of Indion 225 were added into 20 mL of 10 g/L synthetic xylose in the glass flasks. The flasks were shaken in an incubator shaker at 150 rpm for 24 h at different temperatures, i.e., 15, 25, 35, and 45 °C. This operational duration (h) was too long enough for reaching the equilibrium. After equilibrium, the liquid phase was analyzed for the residual xylose concentration by using HPLC. The adsorption capacity of xylose solutions was determined using eq 1.

2.6. Adsorption Kinetics. The adsorption kinetic curves of xylose solutions on the resins were obtained to evaluate the influence of time duration at different temperatures (15, 25, and 35 °C). In the kinetic experiments, 500 mL of mixed synthetic sugar solutions (10 g/L xylose, 0.5 g/L glucose, and 2.5 g/L arabinose) were in contact with 25 g of Amberlite IR120 and Indion 225 in three different flasks. The flasks were shaken in an incubator shaker at 160 rpm for 5 h. The amount of xylose on resin at any duration time 't' was calculated using eq 2[16]

$$q_t = \frac{C_0 V_0 - C_t (V_0 - \sum_{i=1}^{n} V_i)}{m_R} \tag{2}$$

where q_t is the adsorption capacity of xylose at duration time, C_t is the concentration of xylose in solution at duration time,
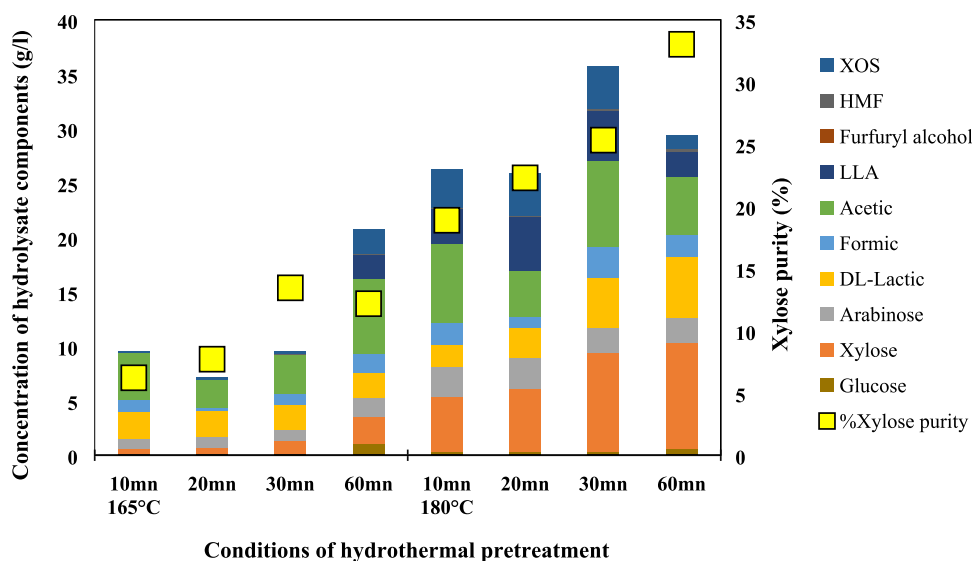
Figure 1. Effect of temperature and time on hydrolysate composition from the hydrothermal process of corncob.

V_0 is the initial volume of solution, and V_i is the sampling volume.

3. RESULTS AND DISCUSSION

3.1. Effect of Hydrothermal Pretreatment on Biochemical Compositions. The hydrolysate compositions of corncob obtained from liquid hot water (LHW) pretreatment at different temperatures and time durations are illustrated in Figure 1. The results indicate that xylose is the major saccharide present in the CC hydrolysate followed by arabinose and glucose. The obtained results are consistent with the results by Chotirotsukon et al.[36] The concentration of xylose increases with increasing temperature and duration of pretreatment. The highest xylose content obtained was 9.705 g/L at 180 °C after 60 min. The obtained results suggest that the LHW triggers the hemicellulose solubilization due to H_3O^+ reacting with hydroxyl groups in hemicellulose in order to release pentose molecules. However, LHW generates several byproducts including acetic acid, 5-hydroxymethylfurfural (HMF), furfuryl alcohol, linoleic acid (LLA), and lactic acid, which are significant inhibitors of the enzymatic hydrolysis and fermentation process.[37,38] The quantity of byproducts generated during pretreatment increases with the increase in temperature and duration as seen in Table 3. These byproducts in particular HMF and furfural affect the enzymatic accessibility and fermentation directly via hindering the active site of the material.

Table 3. Compositions of Solid and Liquid Fractions from Corncob via Hydrothermal Pretreatment at 180 °C, 60 min

composition	solid yield (mg/g biomass)	liquid fraction (g/L)
glucose	442.465	0.578
xylose	n/a	9.705
arabinose	32.038	2.382
DL-lactic	n/a	5.571
formic	n/a	2.028
acetic	n/a	5.380
LLA	n/a	2.207
furfuryl alcohol	n/a	0.042
HMF	n/a	0.223

As seen in Table 3, the concentration of xylose is a major component in the liquid fraction, which could be used as building blocks (in the form of saccharides) for further applications. In addition, the initial concentration of xylose obtained in this study was selected to evaluate the performance of chromatographic ion-exchange separation in the next studies.

3.2. Adsorption Equilibrium. The adsorption equilibrium experiments of three different monosaccharides on the two commercial resins were conducted at 25 °C. The initial concentration of each monosaccharide was approximately 1, 10, 20, and 30 g/L. Under these experimental conditions, xylose, arabinose, and glucose were linearly adsorbed on Amberlite IR120 resin with R^2 values of 0.99, 0.99, and 0.93 for xylose, arabinose, and glucose, respectively. Concerning the Indion 225 resin, three monosaccharides were also linearly related to R^2 values of 0.99, 0.99, and 0.99 for xylose, arabinose, and glucose, respectively, as seen in Figure 2.

All the experimental data fitted well with linear isotherms having the different distribution coefficient (K). It has been reported that the adsorption monosaccharides on cation resin are driven by linear regression.[39] The slope of linear regression represents the constant of adsorption isotherm of different monosaccharides. The distribution coefficient K is represented in Table 4. From Table 4, the distribution coefficient represents the affinity between the adsorbate and the adsorbent. The distribution coefficients (K) of Amberlite IR120 were 90.97, 33.55, and 8.25 L/kg, while the K values of Indion 225 were 54.21, 25.10, and 8.83 L/kg for xylose, arabinose, and glucose, respectively. The high K value of xylose has the strongest affinity with both resins (among the three monosaccharides), indicating that xylose was predicted to be separated last in the chromatographic column.

Moreover, the adsorption capacity of both CER with respect to individual monosaccharides decreased in the order of xylose > arabinose > glucose, respectively. These obtained results can be thus explained by the different size of molecules of each monosaccharides. The separation of neutral sugars is mostly based on differences in molecular sizes and diffusivities. The xylose and arabinose are pentoses, while glucose is a hexose, having larger molecular size than the others.[40] Moreover, the
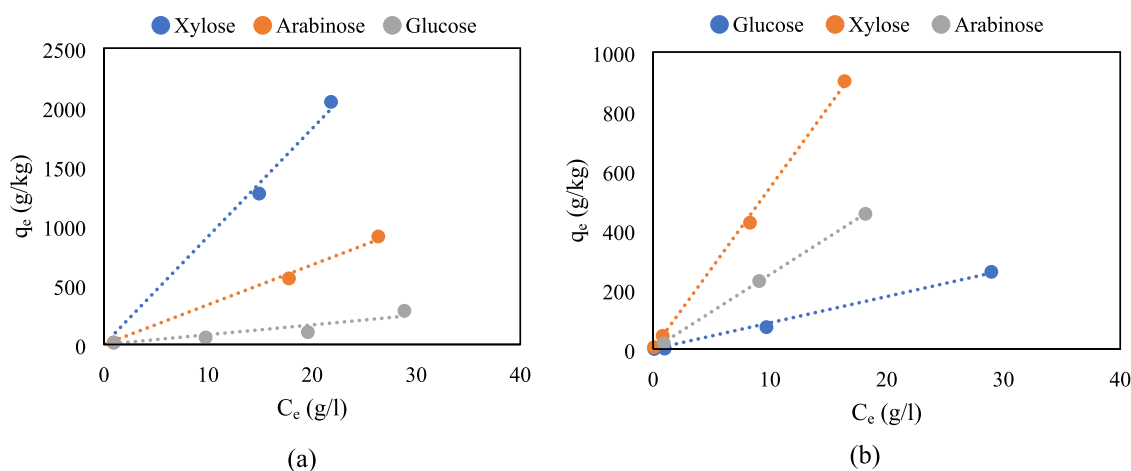
Figure 2. Adsorption isotherms of three monosaccharides on the resins: (a) Amberlite IR120 (b) Indion 225.

Table 4. Distribution Coefficients (K) and Selectivity Factors (α) of Different Resins

type of resin	glucose	R^2	xylose	R^2	arabinose	R^2	Xyl/Glu	Xyl/Ara	Ara/Glu
			K (L/kg)					α	
Amberlite IR120	8.250	0.938	90.967	0.996	33.547	0.998	11.026	2.712	4.066
Indion 225	8.834	0.997	54.268	0.999	25.070	0.999	6.143	2.165	2.838

Table 5. Effect of the Liquid to Solid Ratio on Xylose Purification

type of resin	mass of resin (g)	q_e (mg/g)	suitable liquid/solid ratio (mL/g)	mass of resin (g)	Xyl/Glu	Xyl/Ara	suitable liquid/solid ratio (mL/g)
		10 g/L of xylose			mixed sugars — selectivity factor (α)		
Indion 225	0.5	2.268	100:1	0.5	0.7517	0.9512	20:1
	1.0	0.516		1.0	0.8381	0.9467	
	1.5	1.777		1.5	0.8739	0.9617	
	2.0	1.635		2.0	0.8702	0.9678	
	2.5	1.766		2.5	0.9550	0.9894	
	3.0	1.619		3.0	0.8211	0.9526	
Amberlite IR120	0.5	1.578	20:1	0.5	0.8190	0.9659	20:1
	1.0	1.131		1.0	0.8091	0.9630	
	1.5	1.930		1.5	0.9072	0.9775	
	2.0	2.810		2.0	0.8505	0.9883	
	2.5	5.100		2.5	0.9166	0.9815	
	3.0	0.978		3.0	0.7049	0.9425	

monosaccharide molecules must pass through the resin pores to combine with the resin and be trapped by the pore structure of the resin.[35,41,42] To evaluate the separation efficiency, the selectivity factor (α) defined in eq 3 was determined and the values are presented in Table 4.

$$\alpha = \frac{K_i}{K_j} \tag{3}$$

where K_i and K_j are the different distribution coefficients of each monosaccharide.

The selectivity factor (α) represents the preference of a resin for the target monosaccharides over other monosaccharides present in a mixture of binary sugars. Both Amberlite IR120 and Indion 225 provide a larger xylose/glucose selectivity factor than their xylose/arabinose and arabinose/glucose. These results imply that for both resins a better separation

effect of xylose and glucose could be achieved in comparison to that of xylose/arabinose and arabinose/glucose.

Comparing both the commercial resins, the distribution coefficient K, the capacity of adsorbent, and the selectivity factor indicate that Amberlite IR120 is more suitable for the separation of a mixture of cellulosic sugars from the hydrolysate (in particular xylose).

3.3. Effect of the Liquid to Solid Ratio on Xylose Purification. The xylose concentration obtained from LHW is considered as the initial concentration of xylose for this study in order to determine the quantity of suitable resin for xylose separation. The quantity of adsorbent is one of the crucial parameters for the purification method.

In the current study, the liquid to solid ratio was varied to optimize the amount of cation resin used to separate the hydrolysate-xylose. The suitable quantity of resins would subsequently be used to study the adsorption isotherm and adsorption kinetics at different temperatures. The adsorbent
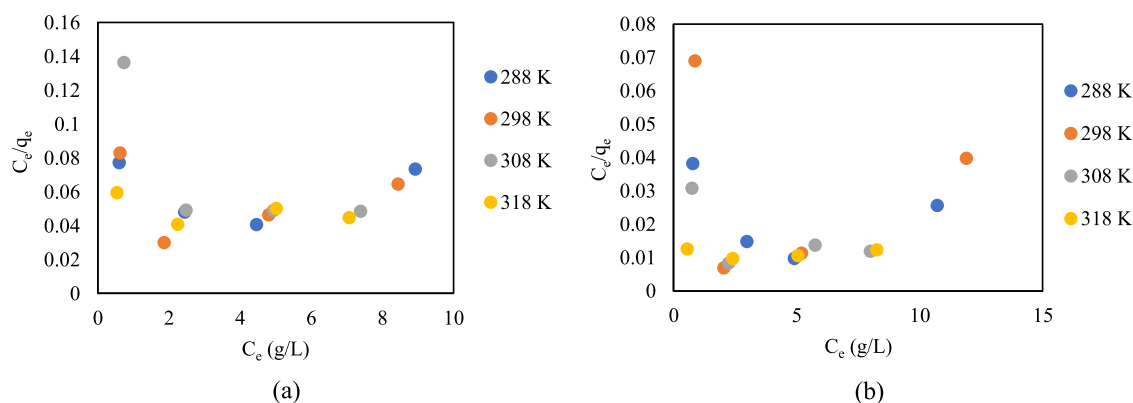
Figure 3. Langmuir adsorption isotherms for both CER at different temperatures: (a) Amberlite IR120 and (b) Indion 225.
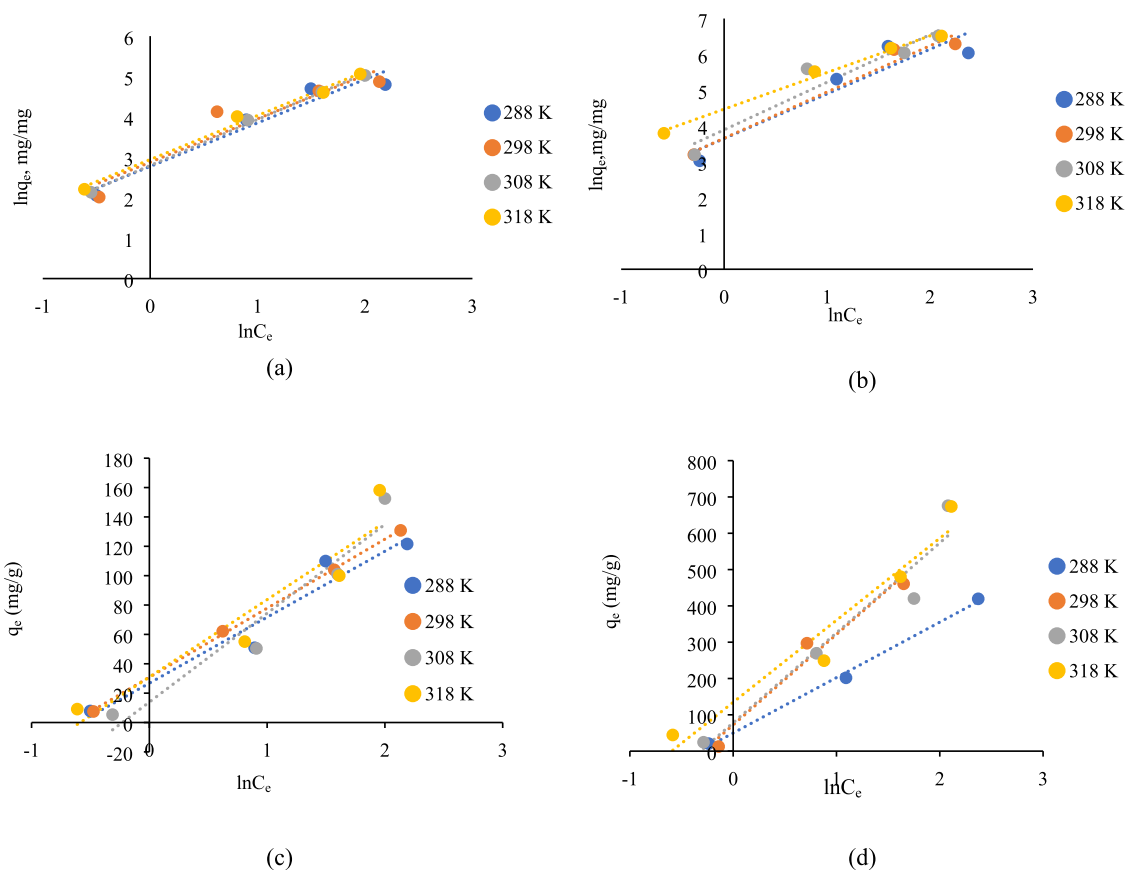

Figure 4. (a, b) Freundlich adsorption isotherms of Amberlite IR120 (a) and Indion 225 (b); (c, d) Temkin adsorption isotherms of Amberlite IR120 (c) and Indion 225 (d) for xylose on both CER at different temperatures.

weight in the range of 0.5−3 g on initial xylose concentration was studied. The suitable liquid to solid ratios of pure xylose and mixed sugar solution are summarized in Table 5, where C_0 is the initial concentration of xylose, i.e., 10.170 g/L, while C_e is the equilibrium concentration (different depending on the quantity of resins used). The highest q_e were 2.268 and 5.100 mg/g for Indion 225 and Amberlite IR120, respectively. For mixed sugars, the highest selectivity factor (α) was at 2.5 g for both CER. The effectiveness of the xylose adsorption decreases with the increasing adsorbent amount. This obtained phenomenon was potentially due to the fact that the number of available adsorption sites increases with an increase in the resin ratio, resulting in an increase in recovery efficiency. On comprehensive consideration of the xylose adsorption

efficiency for both commercial resins, 0.5 and 2.5 g dry resins were selected as the most suitable adsorbent ratio in the further experimental studies.

3.4. Studies on Adsorption Isotherms. Adsorption isotherm is crucial information for understanding how adsorbate interacts with the adsorbent during adsorption. In this study, three commonly used isotherm models, namely, Langmuir, Freundlich, and Temkin, were applied to evaluate the equilibrium data of adsorption for xylose onto two different CER at 15, 25, 35, and 45 °C.[16,43−45]

The first adsorption isotherm is Langmuir isotherm, which was originally applied for gas−solid adsorption.[46] In the current study, the Langmuir isotherm is applied to the liquid−solid adsorption between cation resin and the xylose solution.
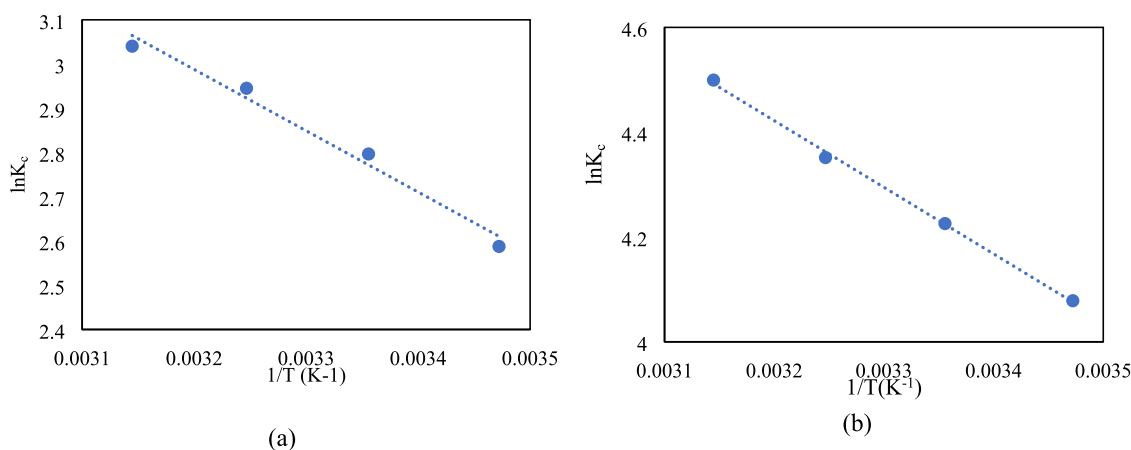
(a)   (b)

Figure 5. Plot of ln K_C versus $1/T$ for xylose adsorption on (a) Amberlite IR120 and (b) Indion 225.

Table 6. Thermodynamic Parameters of Different CER

temp (K)	Amberlite IR120			Indion 225		
	$\Delta G°$ (kJ/mol)	$\Delta H°$ (kJ/mol)	$\Delta S°$ (J/mol·K)	$\Delta G°$ (kJ/mol)	$\Delta H°$ (kJ/mol)	$\Delta S°$ (J/mol·K)
288	−6.230	10.703	58.797	−9.759	10.570	70.589
298	−6.818			−10.465		
308	−7.406			−11.171		
318	−7.994			−11.877		

The Langmuir isotherm typically assumes that the monolayer adsorption occurs onto a special surface containing a finite number of binding sites of uniform strategies of adsorption without interaction between the xylose molecules adsorbed and is not transmigrated on the surface of the adsorbent.[16,43,44] The experimental results obtained indicated that both the CER used in this study do not follow homogeneous adsorption phenomena. Graphically, it is uncharacterized by a linear line as seen in Figure 3. Therefore, it suggests that both CER including Amberlite IR120 and Indion 225 did not show monolayer adsorption.

On the other hand, the Freundlich isotherm model has been used to fit the experimental data. This mathematical model follows an empirical equation. This equation is based on the assumption that multilayer adsorption takes place at the heterogeneous surface and considers the interactions between the adsorbed molecules. The linear equation form of the Freundlich isotherm model[16,46] can be written as (eq 4)

$$\ln q_e = \ln K_F + \frac{1}{n}\ln C_e \tag{4}$$

Graphically, the Freundlich adsorption isotherms of xylose with two different CER are depicted in Figure 4. The adsorption isotherms behave linearly in the investigated concentration range with R^2 close to 1, as observed by different previous studies. K_F and n are the Freundlich constants that can be related to adsorption capacity and adsorption strength. The n value gives an indication of the favorability of the adsorption process. A value of $1/n < 1$ indicates favorable adsorption, whereas $1/n > 1$ indicates cooperative adsorption.[16,47] The obtained K_F in this study for both CER is in the range of 16−19 and 38−87 L/mg for Amberlite IR120 and Indion 225, respectively. Another Freundlich constant is $1/n$ (higher than 1), indicating that both CER show cooperative adsorption. In this study, the $1/n$ is in the range of 1.07−1.14 and 1.02−1.32 for Amberlite

IR120 and Indion 225, respectively, which is higher than 1, indicating that both CER show cooperative adsorption.

Another adsorption isotherm model is Temkin isotherm, which is the model used to describe the interaction between adsorbent−adsorbate. The Temkin model indicates a linear decrease in energy adsorption with surface coverage and considers the interaction between the adsorbate and adsorbent.[16,45] The Temkin isotherm model is defined as eq 5

$$q_e = \frac{RT}{b_T}\ln A_T + \left(\frac{RT}{b_T}\right)\ln C_e \tag{5}$$

Graphically, the adsorption isotherm also behaves linearly in the investigated concentration range with an R^2 value between 0.90−0.99 as seen in Figure 4. The values of the obtained RT/b_T or heat of sorption are in the ranges of 44−60 and 152−249 J/mol for Amberlite IR120 and Indion 225, respectively. The heat of sorption of Amberlite IR120 indicates physisorption, whereas that of Indion 225 indicates chemisorption. However, the Temkin isotherm is generally inappropriate for liquid-phase adsorption.

Among the three-adsorption isotherm models used to describe the interaction between xylose and CER including Amberlite IR120 and Indion 225, the Freundlich isotherm model provides the best fit for adsorption of xylose on both CER. However, the low correlation coefficient (R^2) is an indication that it is not only monolayer adsorption but also the equilibrium isotherms cannot be described by the Langmuir isotherm model.

3.5. Thermodynamic Studies of Both CER. One of the crucial characteristics of both CER is to determine the thermodynamic parameters including $\Delta G°$ (Gibbs free energy), $\Delta H°$ (enthalpy), and $\Delta S°$ (entropy) for understanding the mechanism of adsorption. To determine the thermodynamic parameters related to the adsorption mechanism, the use of the linear Van Hoff equation to describe the
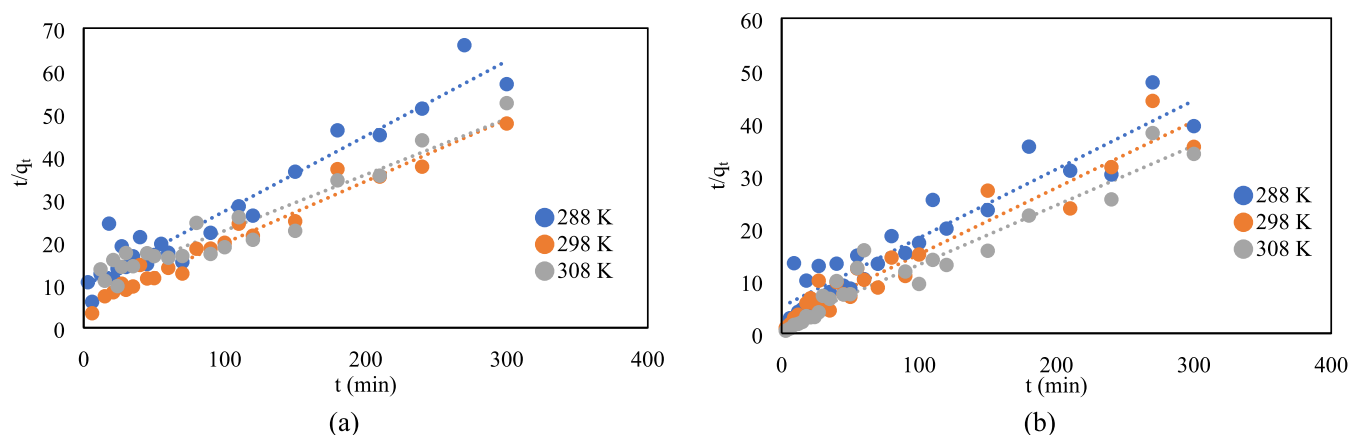
Figure 6. Pseudo-second-order kinetic model of xylose on (a) Amberlite IR120 and (b) Indion 225.

Table 7. Pseudo-Second-Order Parameters of Different CER

temp (K)	$1/T$ (K^{-1})	Amberlite IR120					Indion 225				
		$q_{e,exp}$	$q_{e,cal}$	k_2	R^2	$\ln k_2$	$q_{e,exp}$	$q_{e,cal}$	k_2	R^2	$\ln k_2$
288	0.0035	5.5132	5.6980	0.0032	0.9284	−5.7519	7.5847	7.6336	0.0034	0.8958	−5.6877
298	0.0034	6.2067	6.9156	0.0040	0.9681	−5.5340	8.6790	7.8989	0.0067	0.9304	−5.0108
308	0.0032	6.4383	7.6453	0.0042	0.9177	−5.4726	9.9776	8.8339	0.0073	0.9258	−4.9186

adsorption phenomena of both commercial CER can be described in the form of the following equation eq 6[16,48]

$$\ln K_C = -\frac{\Delta_r H°}{RT} + \frac{\Delta_r S°}{R} \quad (6)$$

The thermodynamic parameters obtained from the slope and intercept of $\ln K_C$ versus $1/T$ have been depicted in Figure 5, where K_C is the thermodynamic equilibrium constant.

The $\Delta G°$ was calculated by the following equation eq 7

$$\Delta G° = \Delta H° - T\Delta S° \quad (7)$$

The thermodynamic parameters calculated using the previous equation are displayed in Table 6. As shown in Table 6, $\Delta G°$ has a negative value indicating that the adsorption process was spontaneous at all temperatures. The value of $\Delta G°$ ranged between (−7.0) − (−8.0) and (−9.0) − (−11.0) kJ/mol for Amberlite IR120 and Indion 225 CER, respectively, and the absolute value was less than 20 kJ/mol, which implied that the adsorption was a physical adsorption process for both the CER.[44] The physical sorption is typically caused by relative weak long-range van der Waals force formed between the adsorbate and CER surface.[49] Furthermore, the decrease in $\Delta G°$ value with increasing temperature indicated that the adsorption of xylose onto both Amberlite IR120 and Indion 225 became favorable at a low temperature. On the other hand, the positive value of $\Delta H°$ indicated that the sorption process of xylose on both CER was endothermic in nature. The adsorption capacity of xylose onto both CER decreased with increasing temperature. The positive value of $\Delta S°$ showed the affinity of the adsorbent toward the adsorbate. It also suggested that the irreversible adsorption increased randomness at the solid/liquid interface with some structural changes in the adsorbent and adsorbate and also that the ion replacement reactions have occurred.[44,50] The obtained thermodynamic parameters in this study were used to determine the inherent energy change of the adsorbent after adsorption and the mechanism involved in xylose adsorption onto both commercial CER.

3.6. Adsorption Kinetic Studies. The adsorption kinetics is important to estimate the rate of the adsorption and evaluate the controlling mechanism of the adsorption process. Moreover, the kinetic behavior of adsorbates on adsorbents has been studied using the effect of time on the adsorption process. In this study, Lagergren's pseudo-first order and pseudo-second-order models were applied as adsorption reaction models to investigate the adsorption kinetic behavior of xylose onto both commercial resins including Amberlite IR120 and Indion 225.[16,45] The adsorption reaction models typically revealed the rate of adsorbate uptake by adsorbents, but they do not indicate the actual cause of adsorption. The equation for Lagergren's pseudo-first order kinetics is as follows eq 8

$$\ln(q_e - q_t) = \ln q_e - k_1 t \quad (8)$$

The values of k_1 and adsorption capacity q_e were computed from the plots of $\ln(q_e - q_t)$ versus t.[51] Comparing the experimental data, i.e., the equilibrium adsorption (q_{exp}) with the calculated results ($q_{e,cal}$), it was obvious that there was no agreement between the values. The correlation coefficient (R^2) for the pseudo-first order indicated poor linearity (nonlinear curve).

On the other hand, the pseudo-second order was applied, which was expressed as eq 9

$$\frac{t}{q_t} = \frac{1}{k_2 q_e^2} + \frac{t}{q_e} \quad (9)$$

where k_2 is the pseudo-second rate constant for the sorption that was obtained by a plot of t/q_e with t.[52] Graphically, it can be observed from Figure 6 and Table 7 that the values of correlation coefficient ($R^2 > 0.90$) for both CER under all operating conditions indicated that the adsorption process followed a pseudo-second-order kinetic model. There was an insignificant error between q_{eexp} and q_{ecal}. The pseudo-second-order kinetic model is generally used to describe the adsorption of adsorbates onto adsorbents where the chemical bonding (interaction) between adsorbates and functional
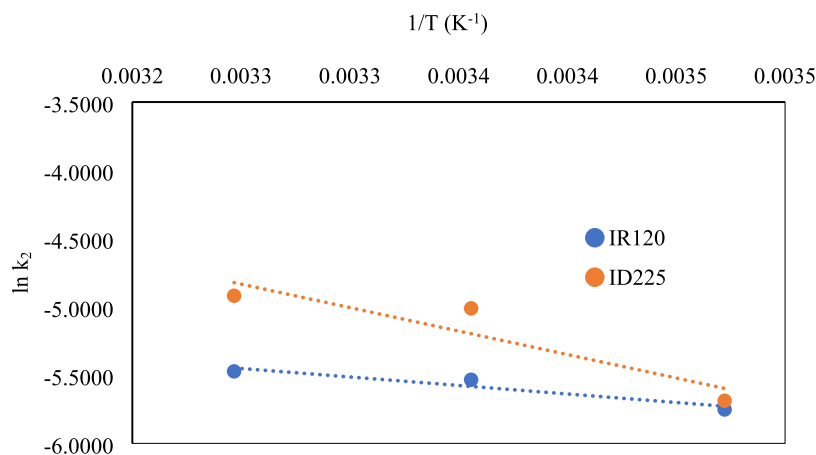
Figure 7. Relationship between $\ln k_2$ and $1/T$ for the adsorption of xylose on both CER.

groups on the surface of adsorbents is responsible for the adsorption capacity of the adsorbent. In this study, the pseudo-second-order kinetic model indicated that the adsorption mechanism between xylose sugar and both CER was a chemisorption process. In addition, the pseudo-second-order kinetic model of both CER suggested that it was a cooperative adsorption process. As xylose is typically an uncharged substance, the electrostatic interactions are unlikely to occur in this study. The cooperative adsorption is typically applicable to physisorptions, as no assumption has been made on the type of interaction.[53] In this study, it would lead to pure physical adsorptions, since the interaction between the adsorbate (xylose) molecules and the adsorbent (CER) surfaces becomes negligible on layers above the adsorbed molecules.[54]

3.7. Determination of Adsorption Activation Energy (E_a). Activation energy is typically the minimum energy required to cause a chemical reaction between an adsorbate and adsorbent. E_a is determined by the second-order rate constant (k_2) obtained from the pseudo-second-order kinetic model. The calculation of activation energy for adsorption processes can be estimated by using the Arrhenius equation as follows eq 10[16,48]

$$\ln k_2 = -\frac{E_a}{RT} + A \tag{10}$$

where k_a = Arrhenius factor A plot of $\ln k_2$ against $1/T$ gives a straight line from which the activation energy (E_a) can be estimated (slope of the linear graph).

Figure 7 illustrates the relationship between $\ln k_2$ and $1/T$ for the adsorption of xylose on both CER. The R^2 values were 0.91 and 0.85 for Ambertlite120 and Indion 225, respectively. According to the previous graphics, the calculated activation energy (E_a) was 10.358 and 28.589 kJ/mol for Amberlite IR120 and Indion 225, respectively. In this study, the obtained E_a indicates the physical nature of the adsorption process for both Amberlite IR120 and Indion 225. The slight difference of E_a of both CER represents the capability of physical attraction that occurred in the adsorption process between the absorbate and adsorbent surface.[53] In this study, the activation energy of adsorption ranging between 5 and 40 kJ/mol is physisorption, while E_a higher than 40 kJ/mol is typically a chemisorption process.[55] These obtained results are consistent with the thermodynamic parameters obtained by previous thermodynamic studies.

4. CONCLUSIONS

An efficient ion-exchange method was presented for the recovery of monosaccharides (xylose) from lignocellulosic hydrolysates. The equilibrium, thermodynamics, and kinetics of both commercial CER including Amberlite 120 and Indion 225 were studied in order to understand the mechanism of xylose adsorption onto the resins. The optimized hydrothermal pretreatment at 180 °C for 60 min provided the highest xylose concentration contained in the hydrolysates. This obtained quantity of xylose in the hydrolysate was used as the initial xylose concentration for equilibrium, thermodynamic, and kinetic studies. The studies of equilibrium revealed that Amberlite IR120 resin was a more suitable resin for xylose purification, compared to Indion 225, with higher selectivity (11.026 and 6.143, respectively). The adsorption isotherm was studied for understanding the interaction between the adsorbate (xylose) and adsorbent, which indicated that it was physical adsorption. Moreover, the thermodynamic studies evaluated the types of the adsorption process, which was physisorption phenomena for both CER (Amberlite IR120 and Indion 225). In addition, the activation energy of adsorption (E_a) (<40 kJ/mol) also indicated the physical nature of the adsorption process for both Amberlite IR120 and Indion 225, which was consistent with the results obtained in the thermodynamic studies.

■ AUTHOR INFORMATION

Corresponding Author

Santi Chuetor − *Department of Chemical Engineering, Faculty of Engineering, King Mongkut's University of Technology North Bangkok (KMUTNB), Bangkok 10800, Thailand; Biorefinery and Process Automation Engineering Centre (BPAEC), King Mongkut's University of Technology North Bangkok, Bangkok 10800, Thailand;* ⊙ orcid.org/0000-0002-3730-7140; Email: santi.c@eng.kmutnb.ac.th

Authors

Jiraporn Phojaroen − *Department of Chemical Engineering, Faculty of Engineering, King Mongkut's University of Technology North Bangkok (KMUTNB), Bangkok 10800, Thailand*

Marisa Raita − *Biorefinery and Bioproducts Research Group, National Center for Genetic Engineering and Biotechnology, Khlong Nueng, Pathumthani 12120, Thailand*

Verawat Champreda − *Biorefinery and Bioproducts Research Group, National Center for Genetic Engineering and Biotechnology, Khlong Nueng, Pathumthani 12120, Thailand;* ⊙ orcid.org/0000-0001-7768-1340

Navadol Laosiripojana − *Joint Graduate School for Energy and Environment (JGSEE), King Mongkut's University of Technology Thonburi (KMUTT), Bangkok 10140, Thailand*

Suttichai Assabumrungrat − *Center of Excellence in Catalysis and Catalytic Reaction Engineering, Department of Chemical Engineering, Faculty of Engineering, Chulalongkorn University, Bangkok 10330, Thailand; Bio-Circular-Green-economy Technology & Engineering Center (BCGeTEC), Faculty of Engineering, Chulalongkorn University, Bangkok 10330, Thailand*

Complete contact information is available at:
https://pubs.acs.org/10.1021/acsomega.3c09246

Notes
The authors declare no competing financial interest.

■ REFERENCES

(1) Chuetor, S.; Barakat, A.; Rouau, X.; Ruiz, T. Analysis of Ground Rice Straw with a Hydro-Textural Approach. *Powder Technol.* **2017**, *310*, 74−79.

(2) Ashokkumar, V.; Venkatkarthick, R.; Jayashree, S.; Chuetor, S.; Dharmaraj, S.; Kumar, G.; Chen, W.-H.; Ngamcharussrivichai, C. Recent Advances in Lignocellulosic Biomass for Biofuels and Value-Added Bioproducts - A Critical Review. *Bioresour. Technol.* **2022**, *344*, No. 126195.

(3) Chuetor, S.; Panakkal, E. J.; Ruensodsai, T.; Cheenkachorn, K.; Kirdponpattara, S.; Cheng, Y.-S.; Sriariyanun, M. Improvement of Enzymatic Saccharification and Ethanol Production from Rice Straw Using Recycled Ionic Liquid: The Effect of Anti-Solvent Mixture. *Bioengineering* **2022**, *9* (3), No. 115, DOI: 10.3390/bioengineering9030115.

(4) Yao, K.; Wu, Q.; An, R.; Meng, W.; Ding, M.; Li, B.; Yuan, Y. Hydrothermal Pretreatment for Deconstruction of Plant Cell Wall: Part II. Effect on Cellulose Structure and Bioconversion. *AIChE J.* **2018**, *64* (6), 1954−1964.

(5) Phojaroen, J.; Jiradechakorn, T.; Kirdponpattara, S.; Sriariyanun, M.; Junthip, J.; Chuetor, S. Performance Evaluation of Combined Hydrothermal-Mechanical Pretreatment of Lignocellulosic Biomass for Enzymatic Enhancement. *Polymers* **2022**, *14* (12), No. 2313, DOI: 10.3390/polym14122313.

(6) Šivec, R.; Grilc, M.; Huš, M.; Likozar, B. Multiscale Modeling of (Hemi)Cellulose Hydrolysis and Cascade Hydrotreatment of 5-Hydroxymethylfurfural, Furfural, and Levulinic Acid. *Ind. Eng. Chem. Res.* **2019**, *58* (35), 16018−16032.

(7) Jakob, A.; Grilc, M.; Teržan, J.; Likozar, B. Solubility Temperature Dependence of Bio-Based Levulinic Acid, Furfural, and Hydroxymethylfurfural in Water, Nonpolar, Polar Aprotic and Protic Solvents. *Processes* **2021**, *9* (6), No. 924, DOI: 10.3390/pr9060924.

(8) Saari, P.; Hurme, M. Process Synthesis Principles in the Chromatographic Separation of Sugars from Biomass Hydrolysates. *Chem. Eng. Technol.* **2011**, *34* (2), 282−288.

(9) Gundupalli, M. P.; Tantayotai, P.; Panakkal, E. J.; Chuetor, S.; Kirdponpattara, S.; Thomas, A. S. S.; Sharma, B. K.; Sriariyanun, M. Hydrothermal Pretreatment Optimization and Deep Eutectic Solvent Pretreatment of Lignocellulosic Biomass: An Integrated Approach. *Bioresour. Technol. Rep.* **2022**, *17*, No. 100957.

(10) Šivec, R.; Likozar, B.; Grilc, M. Surface Kinetics and Transport Phenomena Modelling for Furfural Hydrotreatment over Pd/C in Isopropanol and Tetrahydrofuran. *Appl. Surf. Sci.* **2021**, *541*, No. 148485.

(11) Poletto, P.; Pereira, G. N.; Monteiro, C. R. M.; Pereira, M. A. F.; Bordignon, S. E.; de Oliveira, D. Xylooligosaccharides: Transforming the Lignocellulosic Biomasses into Valuable 5-Carbon Sugar Prebiotics. *Process Biochem.* **2020**, *91*, 352−363.

(12) Krzelj, V.; Liberal, J. F.; Papaioannou, M.; Van Der Schaaf, J.; D'Angelo, M. F. N. Kinetic Model of Xylose Dehydration for a Wide Range of Sulfuric Acid Concentrations. *Ind. Eng. Chem. Res.* **2020**, *59* (26), 11991−12003.

(13) Umai, D.; Kayalvizhi, R.; Kumar, V.; Jacob, S. Xylitol: Bioproduction and Applications-A Review. *Front. Sustainability* **2022**, *3*, No. 826190, DOI: 10.3389/frsus.2022.826190.

(14) Irmak, S.; Canisag, H.; Vokoun, C.; Meryemoglu, B. Xylitol Production from Lignocellulosics: Are Corn Biomass Residues Good Candidates? *Biocatal. Agric. Biotechnol.* **2017**, *11*, 220−223.

(15) Martínez, E. A.; Canettieri, E. V.; Bispo, J. A. C.; Giulietti, M.; De Almeida e Silva, J. B.; Converti, A. Strategies for Xylitol Purification and Crystallization: A Review. *Sep. Sci. Technol.* **2015**, 2087−2098, DOI: 10.1080/01496395.2015.1009115.

(16) Huang, Q.; Lin, X.; Xiong, L.; Huang, C.; Zhang, H.; Luo, M.; Tian, L.; Chen, X. Equilibrium, Kinetic and Thermodynamic Studies of Acid Soluble Lignin Adsorption from Rice Straw Hydrolysate by a Self-Synthesized Macro/Mesoporous Resin. *RSC Adv.* **2017**, *7* (39), 23896−23906.

(17) Gogoi, G.; Hazarika, S. Coupling of Ionic Liquid Treatment and Membrane Filtration for Recovery of Lignin from Lignocellulosic Biomass. *Sep. Purif. Technol.* **2017**, *173*, 113−120.

(18) Heinonen, J.; Tamper, J.; Laatikainen, M.; Sainio, T. Chromatographic Recovery of Monosaccharides and Lignin from Lignocellulosic Hydrolysates. *Chem. Eng. Technol.* **2018**, *41* (12), 2402−2410.

(19) Dou, J.; Heinonen, J.; Vuorinen, T.; Xu, C.; Sainio, T. Chromatographic Recovery and Purification of Natural Phytochemicals from Underappreciated Willow Bark Water Extracts. *Sep. Purif. Technol.* **2021**, *261*, No. 118247.

(20) Chen, K.; Luo, G.; Lei, Z.; Zhang, Z.; Zhang, S.; Chen, J. Chromatographic Separation of Glucose, Xylose and Arabinose from Lignocellulosic Hydrolysates Using Cation Exchange Resin. *Sep. Purif. Technol.* **2018**, *195*, 288−294.

(21) Saari, P.; Heikkila, H.; Hurme, M. Rhamnose, Sucrose, and Xylose on Ion-Exchange Resins. *J. Chem. Eng.* **2010**, *55* (9), 3462−3467.

(22) Han, J.; Xu, B.; Wang, H.; Huang, G.; Zhang, X.; Xu, Y. Enhancing Economic and Environmental Friendliness of Xylonic Acid Bioproduction from Corncob Hydrolysate by the Combined Recycling-Technology of Detoxifying-Resin and Catalyzing-Cell. *Ind. Crops Prod.* **2022**, *188*, No. 115550, DOI: 10.1016/j.indcrop.2022.115550.

(23) Suksom, W.; Wannachai, W.; Boonchiangma, S.; Chanthai, S.; Srijaranai, S. Ion Chromatographic Analysis of Monosaccharides and Disaccharides in Raw Sugar. *Chromatographia* **2015**, *78* (13), 873−879.

(24) Heinonen, J.; Tamper, J.; Laatikainen, M.; Sainio, T. Chromatographic Recovery of Monosaccharides and Lignin from Lignocellulosic Hydrolysates. *Chem. Eng. Technol.* **2018**, *41* (12), 2402−2410.

(25) Dou, J.; Heinonen, J.; Vuorinen, T.; Xu, C.; Sainio, T. Chromatographic Recovery and Purification of Natural Phytochemicals from Underappreciated Willow Bark Water Extracts. *Sep. Purif. Technol.* **2021**, *261*, No. 118247, DOI: 10.1016/j.seppur.2020.118247.

(26) Jiang, Y.; Wang, X.; Wu, Z.; Xu, J.; Hu, L.; Lin, L. Purification of Xylooligosaccharides from Bamboo with Non-Organic Solvent to Prepare Food Grade Functional Sugars. *Results Chem.* **2021**, *3*, No. 100153, DOI: 10.1016/j.rechem.2021.100153.

(27) Heinonen, J.; Tamper, J.; Laatikainen, M.; Sainio, T. Chromatographic Recovery of Monosaccharides and Lignin from Lignocellulosic Hydrolysates. *Chem. Eng. Technol.* **2018**, *41* (12), 2402–2410.

(28) Nobre, C.; Santos, M. J.; Dominguez, A.; Torres, D.; Rocha, O.; Peres, A. M.; Rocha, I.; Ferreira, E. C.; Teixeira, J. A.; Rodrigues, L. R. Comparison of Adsorption Equilibrium of Fructose, Glucose and Sucrose on Potassium Gel-Type and Macroporous Sodium Ion-Exchange Resins. *Anal. Chim. Acta* **2009**, *654* (1), 71–76.

(29) Quirino, J. P.; Alejandro, F. M.; Bissember, A. C. Towards Cleaner Downstream Processing of Biomass Waste Chemical Products by Liquid Chromatography: A Review and Recommendations. *J. Cleaner Prod.* **2020**, No. 119937, DOI: 10.1016/j.jclepro.2019.119937.

(30) Sainio, T.; Kallioinen, M.; Nakari, O.; Mänttäri, M. Production and Recovery of Monosaccharides from Lignocellulose Hot Water Extracts in a Pulp Mill Biorefinery. *Bioresour. Technol.* **2013**, *135*, 730–737.

(31) Leipnitz, M.; Biselli, A.; Merfeld, M.; Scholl, N.; Jupke, A. Model-Based Selection of the Degree of Cross-Linking of Cation Exchanger Resins for an Optimised Separation of Monosaccharides. *J. Chromatogr. A* **2020**, *1610*, No. 460565.

(32) Heinonen, J.; Sainio, T. Electrolyte Exclusion Chromatography Using a Multi-Column Recycling Process: Fractionation of Concentrated Acid Lignocellulosic Hydrolysate. *Sep. Purif. Technol.* **2014**, *129*, 137–149.

(33) Lodi, G.; Pellegrini, L. A.; Aliverti, A.; Torres, B. R.; Bernardi, M.; Morbidelli, M.; Storti, G. Recovery of Monosaccharides from Lignocellulosic Hydrolysates by Ion Exclusion Chromatography. *J. Chromatogr. A* **2017**, *1496*, 25–36.

(34) Chen, K.; Luo, G.; Lei, Z.; Zhang, Z.; Zhang, S.; Chen, J. Chromatographic Separation of Glucose, Xylose and Arabinose from Lignocellulosic Hydrolysates Using Cation Exchange Resin. *Sep. Purif. Technol.* **2018**, *195*, 288–294.

(35) Chen, K.; Hao, S.; Lyu, H.; Luo, G.; Zhang, S.; Chen, J. Ion Exchange Separation for Recovery of Monosaccharides, Organic Acids and Phenolic Compounds from Hydrolysates of Lignocellulosic Biomass. *Sep. Purif. Technol.* **2017**, *172*, 100–106.

(36) Chotirotsukon, C.; Raita, M.; Yamada, M.; Nishimura, H.; Watanabe, T.; Laosiripojana, N.; Champreda, V. Sequential Fractionation of Sugarcane Bagasse Using Liquid Hot Water and Formic Acid-Catalyzed Glycerol-Based Organosolv with Solvent Recycling. *Bioenergy Res.* **2021**, *14*, 135–152.

(37) Slak, J.; Pomeroy, B.; Kostyniuk, A.; Grilc, M.; Likozar, B. A Review of Bio-Refining Process Intensification in Catalytic Conversion Reactions, Separations and Purifications of Hydroxymethylfurfural (HMF) and Furfural. *Chem. Eng. J.* **2022**, *429*, No. 132325, DOI: 10.1016/j.cej.2021.132325.

(38) Liu, Q.; Liu, H.; Gao, D. M. Establishing a Kinetic Model of Biomass-Derived Disaccharide Hydrolysis over Solid Acid: A Case Study on Hierarchically Porous Niobium Phosphate. *Chem. Eng. J.* **2022**, *430* (P2), No. 132756.

(39) Saari, P.; Heikkila, H.; Hurme, M. Rhamnose, Sucrose, and Xylose on Ion-Exchange Resins. *J. Chem. Eng.* **2010**, *55* (9), 3462–3467.

(40) Sjöman, E.; Mänttäri, M.; Nyström, M.; Koivikko, H.; Heikkilä, H. Separation of Xylose from Glucose by Nanofiltration from Concentrated Monosaccharide Solutions. *J. Membr. Sci.* **2007**, *292* (1), 106–115.

(41) Heinonen, J.; Laatikainen, M.; Sainio, T. Chromatographic Fractionation of a Ternary Mixture with an SMB Cascade Process: The Effect of Ion Exchange Resin Cross-Linkage on Separation Efficiency. *Sep. Purif. Technol.* **2018**, *206*, 286–296, DOI: 10.1016/j.seppur.2018.06.016.

(42) Chen, K.; Luo, G.; Lei, Z.; Zhang, Z.; Zhang, S.; Chen, J. Chromatographic Separation of Glucose, Xylose and Arabinose from Lignocellulosic Hydrolysates Using Cation Exchange Resin. *Sep. Purif. Technol.* **2018**, *195*, 288–294.

(43) Trindade, V. N.; Luterbacher, J. S.; Dumesic, J. A.; da Silva, E. A.; Guirardello, R. Adsorption of Water/Glucose Mixture onto Amberlite Resin. *Chem. Eng. Trans.* **2015**, *43*, 607–612.

(44) Zhou, X.; Fan, J.; Li, N.; Qian, W.; Lin, X.; Wu, J.; Xiong, J.; Bai, J.; Ying, H. Adsorption Thermodynamics and Kinetics of Uridine 5′-Monophosphate on a Gel-Type Anion Exchange Resin. *Ind. Eng. Chem. Res.* **2011**, *50* (15), 9270–9279.

(45) Wu, Y. C.; Wei, Y. H.; Wu, H. S. Adsorption and Desorption Behavior of Ectoine Using Dowex HCR-S Ion-Exchange Resin. *Processes* **2021**, *9* (11), No. 2068.

(46) Foo, K. Y.; Hameed, B. H. Insights into the Modeling of Adsorption Isotherm Systems. *Chem. Eng. J.* **2010**, *156*, 2–10.

(47) Chen, K.; Hao, S.; Lyu, H.; Luo, G.; Zhang, S.; Chen, J. Ion Exchange Separation for Recovery of Monosaccharides, Organic Acids and Phenolic Compounds from Hydrolysates of Lignocellulosic Biomass. *Sep. Purif. Technol.* **2017**, *172*, 100–106.

(48) Inglezakis, V. J.; Zorpas, A. A. Heat of Adsorption, Adsorption Energy and Activation Energy in Adsorption and Ion Exchange Systems. *Desalin. Water Treat.* **2012**, *39* (1–3), 149–157.

(49) Sahoo, T. R.; Prelot, B. Adsorption Processes for the Removal of Contaminants from Wastewater: The Perspective Role of Nanomaterials and Nanotechnology. In *Nanomaterials for the Detection and Removal of Wastewater Pollutants*; Bonelli, B.; Freyria, F. S.; Rossetti, I.; Sethi, R., Eds.; Elsevier, 2020; Chapter 7, pp 161–222.

(50) Lin, X.; Huang, Q.; Qi, G.; Xiong, L.; Huang, C.; Chen, X.; Li, H.; Chen, X. Adsorption Behavior of Levulinic Acid onto Microporous Hyper-Cross-Linked Polymers in Aqueous Solution: Equilibrium, Thermodynamic, Kinetic Simulation and Fixed-Bed Column Studies. *Chemosphere* **2017**, *171*, 231–239.

(51) Vadivelan, V.; Kumar, K. V. Equilibrium, Kinetics, Mechanism, and Process Design for the Sorption of Methylene Blue onto Rice Husk. *J. Colloid Interface Sci.* **2005**, *286* (1), 90–100.

(52) Ho, Y. S. Removal of Copper Ions from Aqueous Solution by Tree Fern. *Water Res.* **2003**, *37* (10), 2323–2330.

(53) Liu, S. Cooperative Adsorption on Solid Surfaces. *J. Colloid Interface Sci.* **2015**, *450*, 224–238.

(54) Pourhakkak, P.; Taghizadeh, A.; Taghizadeh, M.; Ghaedi, M.; Haghdoust, S. Fundamentals of Adsorption Technology. In *Adsorption: Fundamental Processes and Applications*; Ghaedi, M., Ed.; Elsevier, 2021; Vol. 33, Chapter 1, pp 1–70.

(55) Unuabonah, E. I.; Adebowale, K. O.; Olu-Owolabi, B. I. Kinetic and Thermodynamic Studies of the Adsorption of Lead (II) Ions onto Phosphate-Modified Kaolinite Clay. *J. Hazard Mater.* **2007**, *144* (1–2), 386–395.